Original Article

Left atrioventricular coupling and left atrial abnormality in patients with acute myocardial infarction with and without hyperglycemia assessed with 3.0T cardiac magnetic resonance imaging feature tracking

Pei-Lun Han[1], Kang Li[1,2,3], Yu Jiang[1], Li Jiang[1], Xin Tang[1], Ying-Kun Guo[4], Yuan Li[1], Zhi-Gang Yang[1]

[1]Department of Radiology and West China Biomedical Big Data Center, West China Hospital, Sichuan University, Chengdu, China; [2]Med-X Center for Informatics, Sichuan University, Chengdu, China; [3]Shanghai Artificial Intelligence Laboratory, Shanghai, China; [4]Department of Radiology, West China Second University Hospital, Sichuan University, Chengdu, China

Contributions: (I) Conception and design: PL Han; (II) Administrative support: ZG Yang, K Li; (III) Provision of study materials or patients: Y Li, ZG Yang; (IV) Collection and assembly of data: PL Han, Y Jiang, L Jiang, X Tang; (V) Data analysis and interpretation: PL Han, Y Li, YK Guo; (VI) Manuscript writing: All authors; (VII) Final approval of manuscript: All authors.

Correspondence to: Yuan Li, MD; Zhi-Gang Yang, MD, PhD. Department of Radiology and West China Biomedical Big Data Center, West China Hospital, Sichuan University, No. 37 Guoxue Xiang, Chengdu 610041, China. Email: dr.liyuan@163.com; yangzg666@163.com.

Background: The relationship between stress hyperglycemia and left atrial (LA) abnormality and left atrioventricular coupling in patients with acute myocardial infarction (AMI) has not been fully explored. This study aimed to assess the additive effect of hyperglycemia on LA phasic function and to investigate the atrioventricular interaction in patients with AMI via cardiac magnetic resonance imaging (MRI).

Methods: This study comprised 120 patients with AMI with admission normoglycemia (aNGL), 88 patients with AMI and admission hyperglycemia (aHGL), and 70 age- and sex-matched controls. LA volume (LAV), LA ejection fraction (LAEF), and LA reservoir/conduit/contraction strain (εs/εe/εa) were measured and compared. Subgroup analysis was performed according to the presence of LA enlargement [LAE; defined as a maximum LAV index (LAVImax) >55 mL/m^2]. Univariate and multivariate linear regression analyses were employed to identify the independent factors related to LA phasic strains.

Results: Compared with controls, patients with AMI had increased LAVI and decreased LAEF and LA strains (all P values <0.05), and the LA reservoir [LA total ejection fraction (LATEF) and εs] and conduit [LA passive ejection fraction (LAPEF) and εe] dysfunction was also present in those without LAE (all P values <0.05). Furthermore, εs and εe were significantly reduced in the aHGL group as compared with the aNGL group (both P values <0.001). After adjustments were made for confounding clinical factors, admission blood glucose level (aBGL) was independently and significantly associated with εs (β=–0.211; P=0.002) and εe (β=–0.215; P=0.001) in patients with AMI. After the introduction of left ventricular (LV) indicators into multivariable regression models, LV global longitudinal strain (GLS) was significantly associated with εs (β=–0.467; P<0.001) and εe (β=–0.455; P<0.001).

Conclusions: Hyperglycemia was found to exacerbate LA reservoir and conduit dysfunction in patients with AMI. aBGL and LV GLS were independent determinants of the εs and the εe, suggesting that attention should be paid not only to glucose monitoring but also to cardiac function indicators.

Keywords: Acute myocardial infarction (AMI); hyperglycemia; left atrial phasic function (LA phasic function); atrioventricular coupling; cardiac magnetic resonance (CMR)

Submitted Aug 22, 2024. Accepted for publication Jan 09, 2025. Published online Feb 18, 2025.
doi: 10.21037/qims-24-1757
View this article at: https://dx.doi.org/10.21037/qims-24-1757

Introduction

Acute myocardial infarction (AMI) is a major cause of morbidity and mortality worldwide (1,2). Stress hyperglycemia is often present in patients with AMI and may increase the risk of adverse cardiovascular outcomes in this population (3,4). Admission blood glucose level (aBGL) is commonly used as a valuable and readily accessible indicator for determining stress hyperglycemia. Clarifying the role of stress hyperglycemia in myocardial abnormalities is of great significance for improving the risk assessment and clinical management of patients with AMI. However, previous studies on myocardial abnormalities in hyperglycemic patients with AMI have mainly focused on left ventricular (LV) structure and function (5-7).

The left atrium is a critical component in modulating LV filling and regulating cardiac output throughout the entire cardiac cycle (8). Atrial enlargement is an important precursor of left atrial (LA) remodeling, which is associated with atrial fibrillation development in AMI (9). Beyond LA size, LA phasic function is being increasingly recognized as an important determinant of cardiovascular events (10). As reported in previous studies (11,12), both AMI and hyperglycemia can induce complex changes in LV function, which may further lead to LA remodeling. Although some studies (13-15) have observed LA damage in AMI via echocardiology and cardiac magnetic resonance imaging (MRI), the potential additive effect of hyperglycemia on LA function among patients with AMI has not been fully explored.

Cardiac MRI can provide a reliable means of depicting cardiac structure and function due to its excellent spatial and temporal resolution (16,17). Similar to those of the left ventricle, the size and function of the left atrium can be quantified using several indices (18-20). Among them, LA strain derived from cardiac MRI feature tracking, which reflects the change in distance from the posterior LA wall to the atrioventricular junction, allows for the sensitive quantification of LA phasic function (21). Therefore, this study aimed to investigate whether hyperglycemia aggravates the impairment of LA function in patients with AMI as indicated by cardiac MRI and to characterize the atrioventricular coupling in AMI. We present this article in accordance with the STROBE reporting checklist (available at https://qims.amegroups.com/article/view/10.21037/qims-24-1757/rc).

Methods

The study was conducted in accordance with the Declaration of Helsinki (as revised in 2013) and was approved by the Biomedical Research Ethics Committee of the West China Hospital of Sichuan University (approval No. 2019-756). The requirement for individual consent was waived due to the retrospective nature of the analysis.

Study population

We retrospectively screened 275 consecutive patients with AMI who underwent enhanced cardiac MRI from January 1, 2012, to July 30, 2023. The diagnosis of AMI was made based on the fourth universal definition of myocardial infarction (22). Patients were excluded if they had coexisting acquired cardiomyopathy, severe valvular disease requiring surgical intervention, congenital heart disease, poor image quality, and missing aBGL information (Figure S1). The control group comprised sex- and age-matched individuals that met the inclusion criteria, which included the absence of dyspnea, chest pain, palpitation, or any other symptoms related to cardiovascular disease, as well as the absence of any abnormalities on cardiac MRI [such as wall motion abnormality, perfusion defect, and myocardial late gadolinium enhancement (LGE)].

Finally, a total of 208 patients (168 males and 40 females; mean age 57±12 years) and 70 controls (51 males and 19 females; mean age 56±13 years) were included. Based on the presence of admission stress hyperglycemia (aBGL of ≥7.8 mmol/L) (23), patients with AMI were classified as admission normoglycemia (aNGL; n=120; 98 males and 22 females) as admission hyperglycemia (aHGL; n=88; 70 males and 18 females).

Cardiac MRI scanning protocol

Cardiac MRI scans were conducted with participants in the supine position via 3.0T whole-body scanners (Tim Trio/

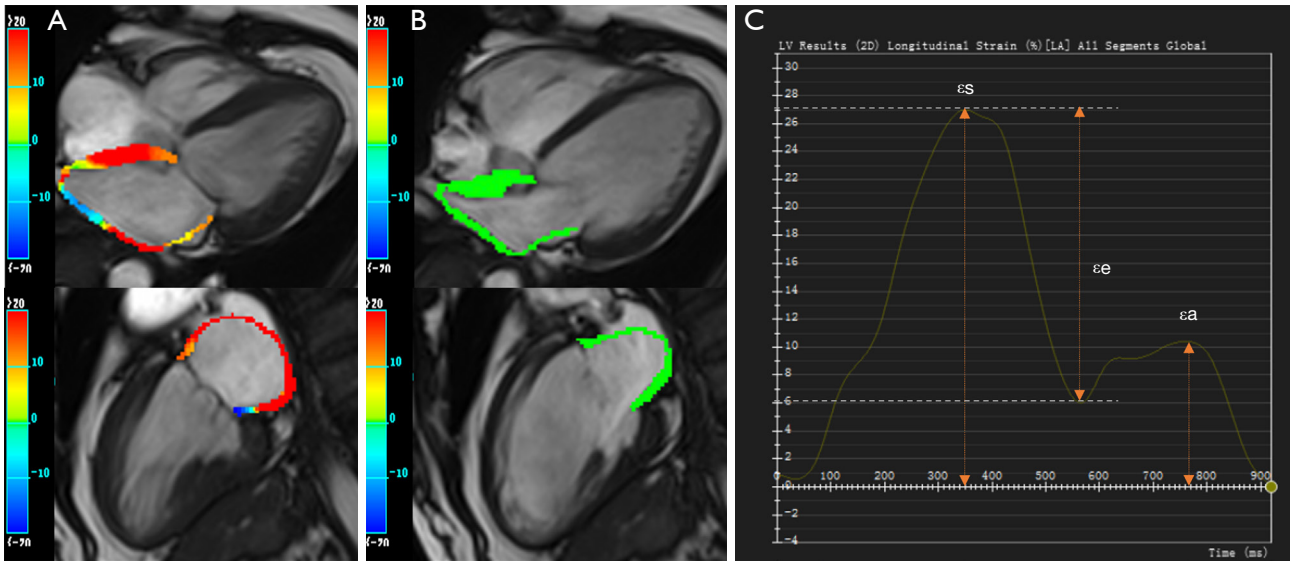

Figure 1 Example images of LA phasic strains in a patient with AMI and hyperglycemia. The images on the left represent pseudocolor cine images in two-chamber and four-chamber long-axis views in the states of (A) maximal and (B) minimal LA volumes, respectively. (C) The image on the right is the LA strain-time curve. LA, left atrial; εs, reservoir strain; εe, conduit strain; εa, booster strain.

MAGNETOM Skyra; Siemens Healthineers, Erlangen, Germany), equipped with a dedicated two-element cardiac-phased array coil and a standard electrocardiography (ECG)-triggering device. Following each survey scan, 8–12 continuous cine images in the short-axis view and two-, three-, and four-chamber cine images in the long-axis view were acquired using a balanced steady-state free-precession sequence [repetition time (TR) =2.8 ms/3.4 ms, echo time (TE) =1.22 ms, flip angle =40°/50°, slice thickness =8 mm, field of view (FOV) =250×300 mm^2/340×285 mm^2, matrix size =208×139/256×166 pixels]. Gadolinium-based contrast agent at a dose of 0.2 mL/kg was injected intravenously at a flow rate of 2.5–3.0 mL/s, followed by a 20-mL saline flush at a flow rate of 3.0 mL/s. After 10–15 minutes, LGE imaging was acquired using a segmented turbo FLASH phase-sensitive inversion recovery sequence (TR =750/512 ms, TE =1.18/1.24 ms, flip angle =20°/40°, slice thickness =8 mm, FOV =240×300/288×360 mm^2, matrix size =256×184/256×125 pixels).

Imaging analysis

Cardiac MRI image analyses were performed on dedicated software (CVI42, Circle Cardiovascular Imaging, Inc., Calgary, Canada) by two experienced radiologists blinded to the patients' basic information. Any disagreement was through discussion.

LA volume (LAV) and function analysis

In the two- and four-chamber cine images, the LA endocardial and epicardial borders were manually delineated at maximal and minimal LAV states, with pulmonary veins and the LA appendage being excluded. Cardiac MRI feature tracking technology was used to automatically track each myocardial voxel in all frames throughout the entire cardiac cycle, with end-diastole used as the reference phase. Subsequently, three phases of LA global longitudinal strain (GLS) were automatically obtained, including LA reservoir strain (εs), conduit strain (εe), and booster strain (εa) (*Figure 1*). Corresponding phasic strain rates, including peak positive strain rate (SRs), peak early negative strain rate (SRe), and late peak negative strain rate (SRa), were also obtained automatically.

LAV analysis was performed using the validated biplane area-length method (24). The maximum LAV (LAVmax), LAV prior to atrial contraction (LAVpre-a), and minimum LAV (LAVmin) were assessed at LV end-systole, LV diastole before LA contraction, and late LV diastole after LA contraction, respectively. LAV index (LAVI) was obtained by indexing LAV to the body surface area (BSA). LA ejection fraction (LAEF), including LA total ejection

fraction (LATEF), LA passive ejection fraction (LAPEF), and LA active ejection fraction (LAAEF) were calculated as volumetric measures of reservoir, conduit, and booster phases, respectively. The formulae for calculation were as follows (25): LATEF = (LAVmax – LAVmin) × 100%/LAVmax; LAPEF = (LAVmax – LAVpre-a) × 100%/LAVmax; LAAEF = (LAVpre-a – LAVmin) × 100%/LAVpre-a.

LV structure and function analysis

The end-diastolic and end-systolic LV endocardial and epicardial contours were manually delineated in serial short-axis slices, and LV end diastolic volume (LVEDV), end systolic volume (LVESV), stroke volume (LVSV), ejection fraction (LVEF), and LV mass were automatically obtained. Following this, LVEDV, LVESV, LVSV, and LV mass were indexed to BSA to obtain the LVEDV index (LVEDVI), LVESV index (LVESVI), LVSV index (LVSVI), and LVM index (LVMI), respectively.

Next, in the three-dimensional feature tracking module, we manually delineated the end-diastolic endocardial and epicardial contours in long-axis two-chamber, four-chamber, and serial short-axis slices. Feature tracking was then performed using the end-diastole phase as the reference phase, and the LV global radial strain (GRS), global circumferential strain (GCS), and GLS were automatically obtained.

Intra- and interobserver reproducibility analysis

We randomly selected 30 participants (20 patients with AMI and 10 controls) to determine the reproducibility of the LA indicators. To evaluate the intraobserver variability, LA indicators were measured once more by the same radiologist after 1 month. To determine the interobserver variability, LA indicators were measured again by a second blinded investigator.

Statistical analysis

The normality of data distributions was assessed using the Kolmogorov-Smirnov test. Continuous variables are reported as the mean ± standard deviation (normally distributed) or as the median with interquartile range (IQR; nonnormally distributed), while categorical variables are reported as frequencies (%). To compare the continuous variables between three groups, one-way analysis of variance followed by the least significant difference (LSD) *post hoc* test or Kruskal-Wallis test was first completed, after which the Mann-Whitney test was performed as appropriate. To compare continuous variables between two groups, the Student's *t*-test or Mann-Whitney test was used as appropriate. To compare categorical variables, Chi-squared tests or the Mann-Whitney test was applied. Pearson or Spearman correlation was applied for correlation analysis. Linear regression analysis was performed to determine the factors related to LA strain. Age, sex, and variables with P<0.1 in univariate analysis were included in the stepwise multivariate linear regression model. The intraclass correlation coefficient (ICC) was used to assess the variability of LA indicators. For all statistical analyses, a two-tailed P value <0.05 was considered statistically significant. All statistical analyses were conducted with SPSS 23.0 (IBM Corp., Armonk, NY, USA) and GraphPad Prism 10 (Dotmatics, Boston, MA, USA).

Results

Baseline clinical characteristics

The baseline characteristics of patients with AMI and controls are summarized in *Table 1*. There was no significant difference in age or sex distribution between controls and patients with AMI (both P values >0.05). Patients with AMI had a significantly higher body mass index, systolic blood pressure, and diastolic blood pressure compared with controls (all P values <0.05). Among the patients with AMI, the aHGL group, as compared with the aNGL group, had a higher prevalence of diabetes and single-vessel disease, as well as higher usage of insulin, biguanides, and sulfonylureas (all P values <0.05). Hemoglobin A1c (HbA1C) and peak troponin were significantly higher in the aHGL group than in the aNGL group (both P values <0.05). There was no significant difference in time from AMI onset to cardiovascular magnetic resonance (CMR) between the aNGL (median 4.00, IQR, 3.00–5.00) and aHGL group (median 4.00, IQR, 2.00–5.00) (P=0.118).

Comparison of cardiac MRI indicators between the patients with AMI and controls

For LA structure and function, both patients with AMI with aNGL and aHGL showed significantly increased LAVI (LAVIpre-a and LAVImin), decreased LAEF (LATEF, LAPEF and LAAEF), decreased LA strain (εs, εe and εa), and decreased LA strain rate (SRs, SRe, and SRa)

Table 1 Baseline demographic and clinical characteristics of the study population

Characteristic	Control (n=70)	AMI with aNGL (n=120)	AMI with aHGL (n=88)	P	P1	P2	P3
Age, years	60.00 (46.00, 65.00)	55.00 (45.25, 65.75)	61.00 (53.00, 65.75)	0.077	0.770	0.124	0.026
Sex				0.350	0.154	0.324	0.701
Female	19 (27.1)	22 (18.3)	18 (20.5)				
Male	51 (72.9)	98 (81.7)	70 (79.5)				
Body mass index, kg/m^2	23.78 (21.49, 25.30)	24.28 (20.76, 27.27)	25.40 (22.11, 29.14)	0.003	0.049	0.001	0.101
Systolic blood pressure, mmHg	115.50 (111.00, 120.00)	123.00 (114.00, 142.75)	127.50 (108.00, 144.25)	<0.001	<0.001	<0.001	0.659
Diastolic blood pressure, mmHg	75.00 (70.00, 78.00)	77.50 (70.00, 87.00)	78.00 (67.00, 91.50)	0.032	0.013	0.032	0.796
Heart rate, bpm	72.00 (64.75, 81.25)	75.25 (66.88, 86.03)	76.00 (68.33, 86.03)	0.204	0.101	0.126	0.955
Cardiovascular risk factors							
Previous/current smoker	–	76 (63.3)	56 (63.6)	–	–	–	0.964
Alcohol consumption	–	52 (43.3)	46 (52.3)	–	–	–	0.202
Hyperlipidemia	–	13 (10.8)	6 (6.8)	–	–	–	0.321
Hypertension	–	55 (45.8)	44 (50.0)	–	–	–	0.552
Diabetes	–	16 (13.3)	37 (42.0)	–	–	–	<0.001
Family history	–	21 (17.5)	9 (10.2)	–	–	–	0.140
Killip functional class				–	–	–	0.883
I	–	81 (67.5)	60 (68.2)				
II	–	23 (19.2)	12 (13.6)				
III	–	13 (10.8)	13 (14.8)				
IV	–	3 (2.5)	3 (3.4)				
Laboratory results							
aBGL, mg/dL	–	113.40 (97.25, 124.56)	184.95 (151.79, 256.73)	–	–	–	<0.001
Peak troponin, ng/L	–	1,672.50 (284.40, 4,592.75)	2,805.00 (852.98, 7,223.25)	–	–	–	0.014
Total cholesterol, mmol/L	–	4.12 (3.59, 4.78)	4.15 (3.62, 4.88)	–	–	–	0.724
Triglycerides, mmol/L	–	1.31 (0.96, 1.77)	1.43 (0.99, 2.26)	–	–	–	0.226
HDL, mmol/L	–	1.11 (0.95, 1.34)	1.13 (0.92, 1.33)	–	–	–	0.793
LDL, mmol/L	–	2.41 (1.95, 3.01)	2.42 (1.92, 2.98)	–	–	–	0.814
eGFR, mL/min/1.73 m^2	–	78.00 (65.00, 90.00)	76.50 (66.67, 92.51)	–	–	–	0.832
HbA1C, mmol/L (n=99)	–	5.95 (5.50, 6.15)	6.90 (5.80, 8.35)	–	–	–	0.001
Number of diseased vessels							
LM	–	10 (8.3)	8 (9.1)	–	–	–	0.848
1 vessel	–	30 (25.0)	10 (11.4)	–	–	–	0.014
2 vessels	–	27 (22.5)	30 (34.1)	–	–	–	0.064
3 vessels	–	48 (40.0)	37 (42.0)	–	–	–	0.767

Table 1 (*continued*)

Table 1 (*continued*)

Characteristic	Control (n=70)	AMI with aNGL (n=120)	AMI with aHGL (n=88)	P	P1	P2	P3
PCI	–	66 (55.0)	60 (68.2)	–	–	–	0.055
Concomitant medication							
ACEI/ARB	–	7 (5.8)	8 (9.1)	–	–	–	0.370
β-blockers	–	7 (5.8)	3 (3.4)	–	–	–	0.632
Calcium-channel blocker	–	23 (19.2)	13 (14.8)	–	–	–	0.408
Diuretics	–	1 (0.8)	3 (3.4)	–	–	–	0.409
Aspirin	–	2 (1.7)	0	–	–	–	0.509
Statin	–	3 (2.5)	0	–	–	–	0.365
Insulin	–	0	9 (10.2)	–	–	–	0.001
Biguanides	–	1 (0.8)	9 (10.2)	–	–	–	0.005
Sulfonylureas	–	1 (0.8)	6 (6.8)	–	–	–	0.048
α-glucosidase inhibitor	–	1 (0.8)	5 (5.7)	–	–	–	0.100
Time from AMI onset to CMR, days	–	4.00 (3.00, 5.00)	4.00 (2.00, 5.00)	–	–	–	0.118

Data are presented as median (interquartile range) or n (%). P: comparison among three groups; P1: comparison between AMI with aNGL and controls; P2: comparison between AMI with aHGL and controls; P3: comparison between AMI with aHGL and AMI with aNGL. AMI, acute myocardial infarction; aNGL, admission normoglycemia; aHGL, admission hyperglycemia; aBGL, admission blood glucose level; HDL, high-density lipoprotein; LDL, low-density lipoprotein; eGFR, estimated glomerular filtration rate; HbA1C, glycosylated hemoglobin A1c; LM, left main; PCI, percutaneous coronary intervention; ACEI, angiotensin-converting enzyme inhibitor; ARB, angiotensin receptor blocker; CMR, cardiac magnetic resonance.

as compared with controls (all P values <0.05) (*Table 2*). Patients with AMI were divided into a group without (n=102) and a group with (n=106) LA enlargement [LAE; defined as LAVImax >55 mL/m^2 (26)]. Patients with LAE showed significantly decreased LAEF and LA strains in all three phases compared with controls (all P values <0.001). For patients without LAE, LA reservoir (LATEF and εs) and conduit (LAPEF and εe) function were also significantly decreased (all P values <0.05) (*Figure 2*).

For LV structure and function, patients with AMI, regardless of glucose status, had significantly increased LVEDVI, LVESVI, and LVMI but significantly decreased LVSVI, LVEF, LV GRS, LV GCS, and LV GLS as compared to controls (all P values <0.05).

Comparison of cardiac MRI indicators between hyperglycemic and normoglycemic patients

Compared with the aNGL group, the aHGL group had significantly decreased εs [median 19.19 (IQR, 15.98–27.44) *vs.* 27.04 (IQR, 16.33–36.85); P=0.003] and εe [median 9.50 (IQR, 6.18–13.40) *vs.* 13.98 (IQR, 7.06–20.58); P=0.002]; however, aHGL had an approximately 16%, decreased εa [median 10.20 (IQR, 6.62–14.32) *vs.* 12.15 (6.40–16.83); P=0.097], but this difference did not reach the statistical significance. LA strain rate did not differ between the two groups (all P values >0.05). In addition, the aHGL group, as compared with the aNGL group, showed significantly decreased GRS [median 18.88 (IQR, 11.65–28.08) *vs.* 26.80 (IQR, 17.61–36.17); P=0.002], GCS (–10.92±4.07 *vs.* –12.49±4.45; P=0.005), and GLS (median –8.55±3.68 *vs.* –10.39±3.65; P<0.001). Infarct size was significantly increased in the aHGL group compared with the aNGL group (30.74±15.06 *vs.* 25.36±15.66; P=0.014).

Associations between aBGL and LA phasic strains in patients with AMI

In patients with AMI, aBGL was significantly correlated with εs (r=–0.239; P<0.001) and εe (r=–0.272; P<0.001) (*Figure 3*). Univariate analysis showed that aBGL was significantly associated with εs (β=–0.239; P=0.001) and εe (β=–0.272; P<0.001) (*Table 3*). After adjustments were made for confounding clinical factors (Model 1), the significant

Table 2 Comparison of cardiac MRI findings among the control, aNGL, and aHGL group

Characteristic	Control (n=70)	AMI with aNGL (n=120)	AMI with aHGL (n=88)	P	P1	P2	P3
LAVI, mL/m^2							
LAVImax	30.60 (24.61, 34.84)	28.49 (20.99, 38.32)	31.70 (23.85, 40.84)	0.434	0.993	0.248	0.269
LAVIpre-a	18.30 (13.68, 23.81)	21.72 (14.95, 30.30)	23.10 (17.56, 30.36)	0.002	0.012	<0.001	0.296
LAVImin	9.26 (6.04, 11.87)	11.58 (6.78, 19.32)	13.49 (10.06, 20.44)	<0.001	0.003	<0.001	0.094
LAEF, %							
LATEF	68.75 (60.35, 74.43)	58.96 (47.42, 65.16)	53.16 (44.39, 64.39)	<0.001	<0.001	<0.001	0.133
LAPEF	34.54 (28.50, 44.23)	22.54 (10.66, 32.61)	21.81 (14.15, 30.74)	<0.001	<0.001	<0.001	0.891
LAAEF	48.54±16.17	44.02±18.44	39.22±17.06	0.004	0.037	<0.001	0.063
LA longitudinal strain, %							
εs	40.40 (24.48, 45.95)	27.04 (16.33, 36.85)	19.19 (15.98, 27.44)	<0.001	<0.001	<0.001	0.003
εe	23.30 (14.40, 30.00)	13.98 (7.06, 20.58)	9.50 (6.18, 13.40)	<0.001	<0.001	<0.001	0.002
εa	15.40 (8.75, 20.05)	12.15 (6.40, 16.83)	10.20 (6.62, 14.32)	0.001	0.022	<0.001	0.097
LA longitudinal strain rate, %							
SRs	1.70 (1.30, 2.23)	1.30 (0.90, 1.78)	1.20 (0.80, 1.50)	<0.001	<0.001	<0.001	0.092
SRe	−2.10 (−3.03, −1.48)	−1.35 (−1.80, −0.80)	−1.20 (−1.70, −0.70)	<0.001	<0.001	<0.001	0.119
SRa	−1.90 (−2.73, −1.38)	−1.55 (−2.00, −1.10)	−1.50 (−1.78, −0.93)	<0.001	<0.001	<0.001	0.216
LVEDVI, mL/m^2	73.56 (65.10, 84.65)	83.57 (67.88, 99.34)	81.19 (65.99, 103.46)	<0.001	<0.001	0.014	0.756
LVESVI, mL/m^2	25.64 (21.42, 31.61)	41.28 (30.38, 59.11)	41.00 (31.49, 62.82)	<0.001	<0.001	<0.001	0.704
LVSVI, mL/m^2	47.92 (41.58, 54.29)	39.23 (31.06, 48.04)	36.57 (27.77, 45.54)	<0.001	<0.001	<0.001	0.205
LVEF, %	63.70 (61.53, 67.93)	49.41 (36.83, 57.04)	45.79 (36.38, 54.55)	<0.001	<0.001	<0.001	0.201
LVMI, g/m^2	46.38 (38.64, 57.80)	56.70 (45.94, 70.08)	55.90 (49.22, 68.94)	<0.001	<0.001	<0.001	0.913
LV GRS	34.33 (31.11, 38.83)	26.80 (17.61, 36.17)	18.88 (11.65, 28.08)	<0.001	<0.001	<0.001	0.002
LV GCS	−19.92±2.42	−12.49±4.45	−10.92±4.07	<0.001	<0.001	<0.001	0.008
LV GLS	−14.56±3.10	−10.39±3.65	−8.55±3.68	<0.001	<0.001	<0.001	<0.001
Infarct size, % of LV	–	25.36±15.66	30.74±15.06	–	–	–	0.014
Infarct territory							
Anterior	–	35 (29.2)	29 (33.0)	–	–	–	0.559
Inferior	–	50 (41.7)	34 (38.6)	–	–	–	0.660
Interventricular septum	–	71 (59.2)	55 (62.5)	–	–	–	0.627
Lateral	–	34 (28.3)	29 (33.0)	–	–	–	0.474
Transmural infarction	–	35 (29.2)	29 (33.0)	–	–	–	0.559

Data are presented as mean ± standard deviation, median (interquartile range), or n (%). P: comparison among three groups; P1: comparison between AMI with aNGL and controls; P2: comparison between AMI with aHGL and controls; P3: comparison between AMI with aHGL and AMI with aNGL. MRI, magnetic resonance imaging; aNGL, admission normoglycemia; aHGL, admission hyperglycemia; AMI, acute myocardial infarction; LAVI, left atrial volume index; LAVImax, maximum left atrial volume index; LAVIpre-a, left atrial volume index just before left atrial contraction; LAVImin, minimum left atrial volume index; LAEF, left atrial ejection fraction; LATEF, left atrial total emptying fraction; LAPEF, left atrial passive emptying fraction; LAAEF, left atrial active emptying fraction; LA, left atrial; εs, reservoir strain; εe, conduit strain; εa, booster strain; SRs, peak positive strain rate; SRe, peak early negative strain rate; SRa, peak late negative strain rate; LVEDVI, left ventricular end diastolic volume index; LVESVI, left ventricular end systolic volume index; LVSVI, left ventricular stroke volume index; LVEF, left ventricular ejection fraction; LVMI, left ventricular mass index; LV, left ventricular; GRS, global radial strain; GCS, global circumferential strain; GLS, global longitudinal strain.

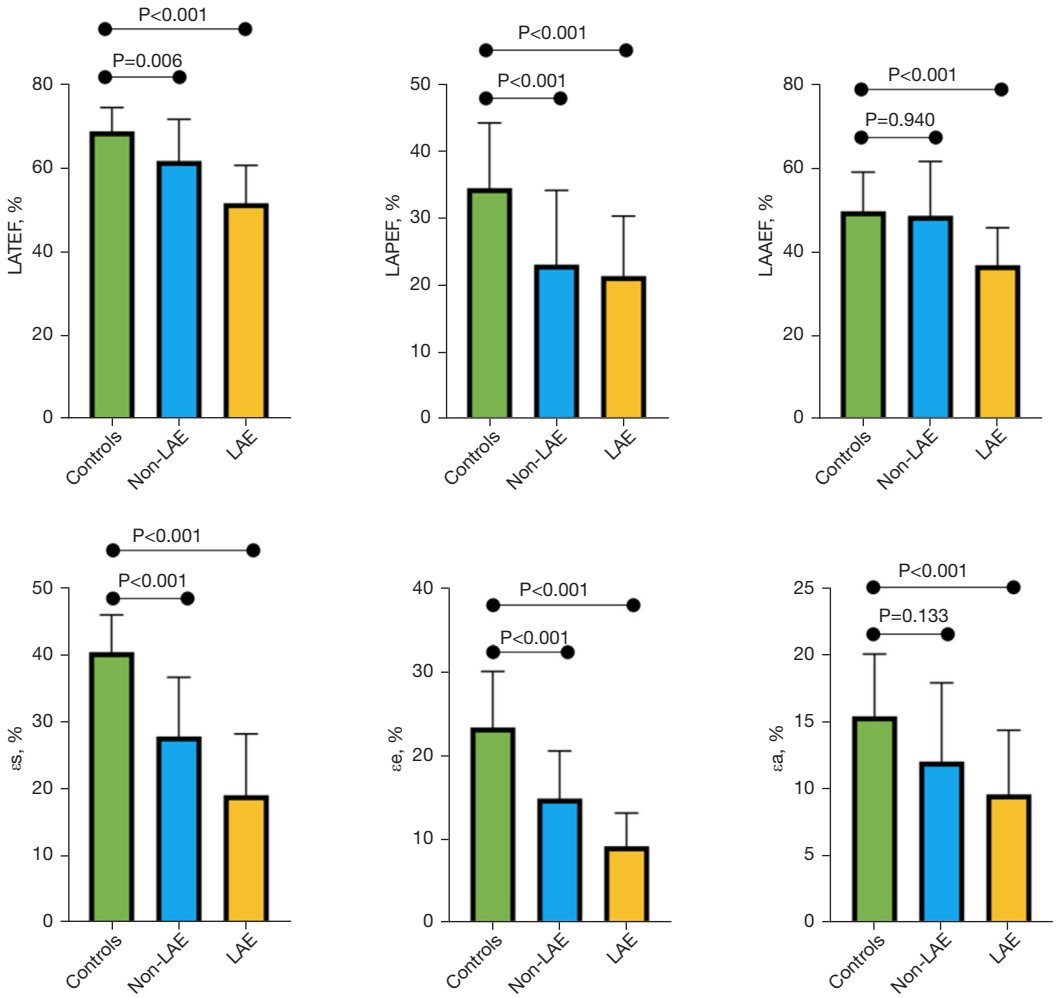

Figure 2 Comparison of LA function between controls, patients with AMI without LAE, and patients with AMI with LAE. LATEF, left atrial total emptying fraction; LAPEF, left atrial passive emptying fraction; LAAEF, left atrial active emptying fraction; εs, reservoir strain; εe, conduit strain; εa, booster strain; LAE, left atrial enlargement; LA, left atrial; AMI, acute myocardial infarction.

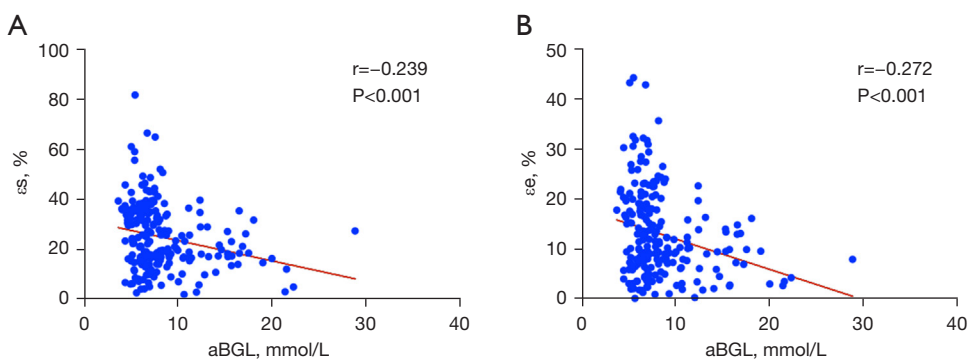

Figure 3 Correlations between aBGL and LA (A) reservoir and (B) conduit strain. εs, reservoir strain; εe, conduit strain; aBGL, admission blood glucose level; LA, left atrial.

Table 3 Univariate and multivariate linear regression of LA longitudinal strain in all patients with AMI

Characteristic	εs						εe					
	Univariable		Model 1 (R^2=0.103)		Model 2 (R^2=0.248)		Univariable		Model 1 (R^2=0.192)		Model 2 (R^2=0.356)	
	β	P	β	P	β	P	β	P	β	P	β	P
Age	−0.201	0.004	−0.211	0.002	−0.145	0.018	−0.355	<0.001	−0.303	<0.001	−0.284	<0.001
Sex	−0.069	0.325	–	–	–	–	−0.012	0.861	–	–	–	–
HR	−0.192	0.006	−0.186	0.005	–	–	−0.202	0.003	−0.188	0.003	–	–
SBP	0.102	0.143	–	–	–	–	0.022	0.757	–	–	–	–
DBP	0.067	0.336	–	–	–	–	0.004	0.954	–	–	–	–
Diabetes	−0.198	0.004	–	–	–	–	−0.248	<0.001	–	–	−0.129	0.024
aBGL	−0.239	0.001	−0.211	0.002	–	–	−0.272	<0.001	−0.215	0.001	–	–
Peak troponin	−0.075	0.283	–	–	–	–	−0.075	0.284	–	–	–	–
Infarct size	−0.198	0.004	–	–	–	–	−0.168	0.015	–	–	–	–
eGFR	−0.001	0.985	–	–	–	–	−0.038	0.584	–	–	–	–
LVEDVI	−0.231	0.001	–	–	–	–	−0.177	0.010	–	–	–	–
LVESVI	−0.325	<0.001	–	–	–	–	−0.281	<0.001	–	–	–	–
LVSVI	0.248	<0.001	–	–	–	–	0.270	<0.001	–	–	–	–
LVEF	0.394	<0.001	–	–	–	–	0.370	<0.001	–	–	–	–
LVMI	−0.060	0.387	–	–	–	–	−0.059	0.397	–	–	–	–
LV GRS	0.424	<0.001	–	–	–	–	0.434	<0.001	–	–	–	–
LV GCS	−0.436	<0.001	–	–	–	–	−0.442	<0.001	–	–	–	–
LV GLS	−0.484	<0.001	–	–	−0.467	<0.001	−0.512	<0.001	–	–	−0.455	<0.001

Model 1 adjusted for age, sex, and clinical factors with P<0.1 in the univariate analysis; Model 2 adjusted for age, sex, and clinical factors and LV indicators with P<0.1 in the univariate analysis. LA, left atrial; AMI, acute myocardial infarction; εs, reservoir strain; εe, conduit strain; HR, heart rate; SBP, systolic blood pressure; DBP, diastolic blood pressure; aBGL, admission blood glucose level; eGFR, estimated glomerular filtration rate; LVEDVI, left ventricular end diastolic volume index; LVESVI, left ventricular end systolic volume index; LVSVI, left ventricular stroke volume index; LVEF, left ventricular ejection fraction; LVMI, left ventricular mass index; LV, left ventricular; GRS, global radial strain; GCS, global circumferential strain; GLS, global longitudinal strain.

associations between aBGL and εs (β=−0.211; P=0.002) and εe (β=−0.215; P=0.001) remained. Results regarding the relationship between aBGL, infarct size, and LV strain are shown in Figure S2 and Table S1.

Correlations between LV global strain and LA phasic strains in patients with AMI

As shown in *Figure 4*, LV global strains (GRS, GCS, and GLS) were significantly correlated with εs and εe (all P values <0.001). Univariate analysis showed that GRS, GCS, and GLS were significantly associated with εs (GRS: β=0.424, P<0.001; GCS: β=−0.436, P<0.001; GLS: β=−0.484, P<0.001) and εe (GRS: β=0.434, P<0.001; GCS: β=−0.442, P<0.001; GLS: β=−0.512, P<0.001). After cardiac MRI indicators were introduced into the multivariate regression models (Model 2), only GLS demonstrated significant associations with εs (β=−0.467; P<0.001) and εe (β=−0.455; P<0.001).

Reproducibility

Cardiac MRI-derived LA structure and function indicators showed excellent intra- and interobserver reproducibility (all ICCs >0.9). The ICCs for LAVI, LAEF, and LA phasic strain are summarized in *Table 4*.

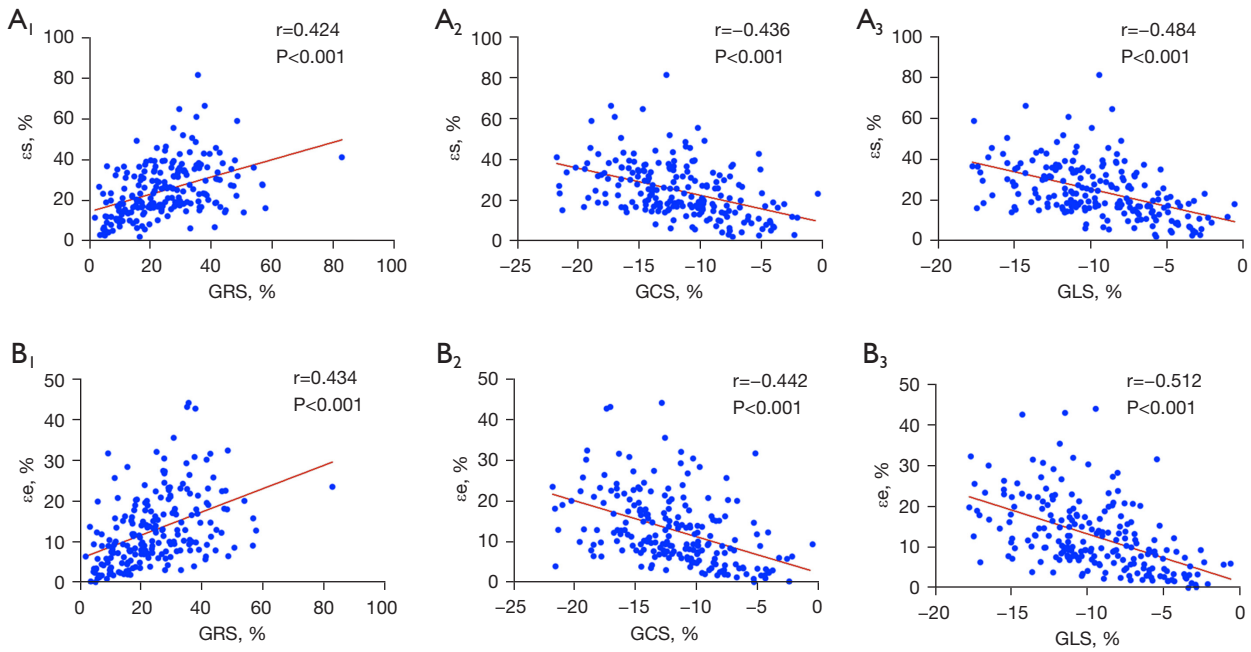

Figure 4 Interaction between LV global strain and LA strain. (A1-A3) Linear regression analysis of GRS, GCS, GLS, and εs. (B1-B3) Linear regression analysis of GRS, GCS, GLS, and εe. GRS, global radial strain; GCS, global circumferential strain; GLS, global longitudinal strain; εs, reservoir strain; εe, conduit strain.

Table 4 Inter- and intraobserver variability of CMR-derived LA structure and function indicators

Parameter	Intraobserver (n=30)		Interobserver (n=30)	
	ICC	95% CI	ICC	95% CI
LAVI, mL/m^2				
LAVImax	0.998	0.995–0.999	0.998	0.995–0.999
LAVIpre-a	0.997	0.994–0.999	0.997	0.993–0.998
LAVImin	0.996	0.992–0.998	0.995	0.989–0.997
LAEF, %				
LATEF	0.976	0.950–0.988	0.969	0.936–0.985
LAPEF	0.953	0.904–0.977	0.958	0.915–0.980
LAAEF	0.960	0.917–0.981	0.952	0.901–0.977
LA longitudinal strain, %				
εs	0.987	0.972–0.994	0.986	0.971–0.993
εe	0.980	0.959–0.990	0.980	0.958–0.990
εa	0.964	0.926–0.983	0.957	0.912–0.979

CMR, cardiac magnetic resonance; LA, left atrial; ICC, intraclass correlation coefficient; 95% CI, 95% confidence interval; LAVI, left atrial volume index; LAVImax, maximum left atrial volume index; LAVIpre-a, left atrial volume index just before left atrial contraction; LAVImin, minimum left atrial volume index; LAEF, left atrial ejection fraction; LATEF, left atrial total emptying fraction; LAPEF, left atrial passive emptying fraction; LAAEF, left atrial active emptying fraction; LA, left atrial; εs, reservoir strain; εe, conduit strain; εa, booster strain.

Discussion

This study adds knowledge to the existing literature on LA functional differences in patients with AMI with and without hyperglycemia and that on atrioventricular coupling in patients following AMI. Our data revealed the following: (I) compared with controls, LA function was decreased in patients with AMI, even those with normal LA volume. (II) Among patients with AMI, LA dysfunction was worse in hyperglycemic individuals, and aBGL was an independent factor correlated with LA strains. (III) LV global strain was correlated with LA phasic strain in patients with AMI, most notably LV longitudinal strain.

LA phasic dysfunction in AMI

The operation of the left atrium is marked by three phases (25). During the LA reservoir phase, the myocytes in the left atrium stretches to receive blood via the pulmonary veins, which typically represents LA compliance. In the subsequent conduit phase, blood streams divert passively into the left ventricle from the left atrium. In the final booster pump phase, the LA contracts actively to pump blood into the left ventricle, which represents the inherent contractility of the LA myocardium. In agreement with previous studies that evaluated LA structure and function using echocardiography and cardiac MRI (12-14), the cardiac MRI results in this study revealed phasic LA morphological and functional abnormalities in patients with AMI. Atrial damage in myocardial infarction has mainly been considered to be a secondary event of ventricular dysfunction since ischemic injury primarily affects the ventricles. The systemic effects during myocardial infarction, such as increased activation of the sympathetic nervous system and of inflammatory pathways, also damage the atrium. Moreover, direct hypoxic damage caused by the concomitant atrial infarctions (incidence 0.7–42%), which lead to atrial structural changes and dysfunction, cannot be ignored (27).

In addition, we found that LAEF and LA longitudinal strains of all three phases were significantly reduced, even in patients with AMI with normal LA size. This suggests that functional changes in AMI may precede morphological alterations. LA functional indicators can detect LA remodeling with sensitivity and is superior to morphological indicators. Therefore, in the management of patients with AMI, even those with normal LA size, close attention should be paid to the indicators of LA function, including LAEF and LA strains.

Hyperglycemia aggravated LA dysfunction in patients with AMI

It has been reported that 29–38% of patients with AMI also have admission stress hyperglycemia (28,29). Hyperglycemic patients with AMI have an increased mortality compared with normoglycemic ones (28). Additionally, this negative association also exists for cardiovascular complications. In our results, LA strains were significantly reduced in hyperglycemic patients with AMI as compared with those with normoglycemia, and aBGL was an independent determinant of LA strains. Stress hyperglycemia has been shown to induce LV dysfunction through multiple pathways such as increased infarct size and compromise myocardial perfusion (23,30-32), which may lead to the reduction of the atrial function given the tight relationship between LV and LA (33,34). In addition, the cardiotoxic effects of stress hyperglycemia, which includes endothelial function, oxidative stress, production of leukocyte adhesion molecules, platelet aggregation, and activation of the coagulation cascade, may directly impact the LA myocardium (27,30,32). Hyperglycemia can lead to elevated LA pressure, which may contribute to diastolic dysfunction and increased risk of atrial fibrillation in patients with AMI (35). Our results also showed that hyperglycemic patients with AMI showed significantly decreased LA strain as compared with normoglycemic patients, although LAEF was not significantly different. This may reflect the higher sensitivity of cardiac MRI feature tracking for detecting myocardial dysfunction, which helps in the early identification and early optimization of treatment. Additionally, in our study, only 42.0% of hyperglycemic patients were identified as diabetic, which aligns with previous research suggesting that hyperglycemia should be considered an additional risk factor (36).

Furthermore, when AMI was combined with hyperglycemia, LA reservoir and conduit strains decreased significantly, whereas LA booster strain decreased slightly. LA reservoir function reflects the LA filling during LV systole, and the reduction of LA reservoir strain may indicate marked impairment of atrial compensatory capacity for hyperglycemic patients with AMI (37). Previous studies have demonstrated that different degrees of LV diastolic dysfunction can influence the different phases of LA function. In patients with mild LV diastolic dysfunction, LA conduit function is impaired, and LA

pump booster function is enhanced to compensate for a deceased LA emptying volume (38,39). This mechanism no longer operates when the severity of diastolic dysfunction increases (39). An echocardiography study (40) reported strong correlations between LV diastolic function and LA conduit and reservoir function, but not with LA booster function, which is consistent with our results. Therefore, our findings suggest that LA booster function may not be a good metric of LA functional capacity.

Atrioventricular coupling in patients following AMI

We further found that LA function injury is associated with LV dysfunction in patients with AMI, and there were correlations between LA and LV strains, especially GLS. Longitudinal myocardial movement is essential to the contraction of the left ventricle (33). During systole, contraction of the longitudinal myocardial fiber of the left ventricle results in the longitudinal stretching of the LA. Interestingly, when LV strains were introduced into the regression models, the correlations between aBGL and LA strains were lost. This might be because of the strong mechanical connection between the atrium and ventricle (20). Thus, clinicians should not only monitor glucose level but also cardiac function indicators in patients with AMI.

Limitations

There were certain limitations to this study which should be acknowledged. First, we employed a single-center study, and thus selection bias could not be avoided. Second, our analysis of LA deformation was limited to longitudinal strains because the reproducibility of the radial strain is poor (41). Third, the dynamic changes of glucose level were not monitored. Further studies will be conducted to investigate the impact of glycemic control and dynamic changes in blood glucose on subclinical cardiac dysfunction. Finally, several factors affect cardiac structure and function in patients with AMI, including gender (42), hypertension (43), and obesity (44). As they would require many studies to examine, we will stratify them individually in future research.

Conclusions

LA reservoir, conduit, and booster pump functions were found to be compromised in patients with AMI, even in those with normal LA size. Hyperglycemia aggravated the impairment of LA reservoir and conduit functions in patients with AMI. aBGL and GLS were independent factors associated with LA reservoir and conduit strains. Therefore, in patients with AMI with admission stress hyperglycemia, both the monitoring of glucose levels and cardiac function is necessary.

Acknowledgments

None.

Footnote

Reporting Checklist: The authors have completed the STROBE reporting checklist. Available at https://qims.amegroups.com/article/view/10.21037/qims-24-1757/rc

Funding: This work was supported by the National Natural Science Foundation of China (No. 82371925); the National Key Research and Development Program of China (Nos. 2020YFB1711500 and 2020YFB1711503); the 1·3·5 Project for Disciplines of Excellence, West China Hospital, Sichuan University (Nos. ZYYC21004 and ZYGD23019); and the Sichuan Province Science and Technology Support Program (Nos. 2022NSFSC0828 and 2024NSFSC1788).

Conflicts of Interest: All authors have completed the ICMJE uniform disclosure form (available at https://qims.amegroups.com/article/view/10.21037/qims-24-1757/coif). The authors have no conflicts of interest to declare.

Ethical Statement: The authors are accountable for all aspects of the work in ensuring that questions related to the accuracy or integrity of any part of the work are appropriately investigated and resolved. This study was conducted in accordance with the Declaration of Helsinki (as revised in 2013) and was approved by the Biomedical Research Ethics Committee of the West China Hospital of Sichuan University (approval No. 2019-756). The requirement for individual consent was waived due to the retrospective nature of the analysis.

References

1. Yeh RW, Sidney S, Chandra M, Sorel M, Selby JV, Go AS. Population trends in the incidence and outcomes of acute myocardial infarction. N Engl J Med 2010;362:2155-65.
2. Benjamin EJ, Muntner P, Alonso A, Bittencourt MS, Callaway CW, Carson AP, et al. Heart Disease and Stroke Statistics-2019 Update: A Report From the American Heart Association. Circulation 2019;139:e56-e528.
3. Wei QC, Chen YW, Gao QY, Ren KD, Liu YB, He F, Shi JT, Jiang J. Association of stress hyperglycemia with clinical outcomes in patients with ST-elevation myocardial infarction undergoing percutaneous coronary intervention: a cohort study. Cardiovasc Diabetol 2023;22:85.
4. Zhang Y, Guo L, Zhu H, Jiang L, Xu L, Wang D, Zhang Y, Zhao X, Sun K, Zhang C, Zhao W, Hui R, Gao R, Wang J, Yuan J, Xia Y, Song L. Effects of the stress hyperglycemia ratio on long-term mortality in patients with triple-vessel disease and acute coronary syndrome. Cardiovasc Diabetol 2024;23:143.
5. Ishihara M, Inoue I, Kawagoe T, Shimatani Y, Kurisu S, Nishioka K, Umemura T, Nakamura S, Yoshida M. Impact of acute hyperglycemia on left ventricular function after reperfusion therapy in patients with a first anterior wall acute myocardial infarction. Am Heart J 2003;146:674-8.
6. Bo K, Li W, Zhang H, Wang Y, Zhou Z, Gao Y, Sun Z, Lian J, Wang H, Xu L. Association of stress hyperglycemia ratio with left ventricular function and microvascular obstruction in patients with ST-segment elevation myocardial infarction: a 3.0 T cardiac magnetic resonance study. Cardiovasc Diabetol 2024;23:179.
7. Han PL, Li K, Jiang Y, Gao Y, Guo YK, Yang ZG, Li Y. Additive effect of admission hyperglycemia on left ventricular stiffness in patients following acute myocardial infarction verified by CMR tissue tracking. Cardiovasc Diabetol 2024;23:210.
8. Thomas L, Abhayaratna WP. Left Atrial Reverse Remodeling: Mechanisms, Evaluation, and Clinical Significance. JACC Cardiovasc Imaging 2017;10:65-77.
9. Luo J, Xu S, Li H, Li Z, Liu B, Qin X, Gong M, Shi B, Wei Y. Long-term impact of new-onset atrial fibrillation complicating acute myocardial infarction on heart failure. ESC Heart Fail 2020;7:2762-72.
10. Chirinos JA, Sardana M, Ansari B, Satija V, Kuriakose D, Edelstein I, Oldland G, Miller R, Gaddam S, Lee J, Suri A, Akers SR. Left Atrial Phasic Function by Cardiac Magnetic Resonance Feature Tracking Is a Strong Predictor of Incident Cardiovascular Events. Circ Cardiovasc Imaging 2018;11:e007512.
11. Garg P, Crandon S, Swoboda PP, Fent GJ, Foley JRJ, Chew PG, Brown LAE, Vijayan S, Hassell MECJ, Nijveldt R, Bissell M, Elbaz MSM, Al-Mohammad A, Westenberg JJM, Greenwood JP, van der Geest RJ, Plein S, Dall'Armellina E. Left ventricular blood flow kinetic energy after myocardial infarction - insights from 4D flow cardiovascular magnetic resonance. J Cardiovasc Magn Reson 2018;20:61.
12. Hombach V, Grebe O, Merkle N, Waldenmaier S, Höher M, Kochs M, Wöhrle J, Kestler HA. Sequelae of acute myocardial infarction regarding cardiac structure and function and their prognostic significance as assessed by magnetic resonance imaging. Eur Heart J 2005;26:549-57.
13. Dogan C, Ozdemir N, Hatipoglu S, Bakal RB, Omaygenc MO, Dindar B, Candan O, Emiroglu MY, Kaymaz C. Relation of left atrial peak systolic strain with left ventricular diastolic dysfunction and brain natriuretic peptide level in patients presenting with ST-elevation myocardial infarction. Cardiovasc Ultrasound 2013;11:24.
14. Yurdakul S, Aytekin S. Left atrial mechanical functions in patients with anterior myocardial infarction: a velocity vector imaging-based study. Kardiol Pol 2013;71:1266-72.
15. Leng S, Ge H, He J, Kong L, Yang Y, Yan F, Xiu J, Shan P, Zhao S, Tan RS, Zhao X, Koh AS, Allen JC, Hausenloy DJ, Mintz GS, Zhong L, Pu J. Long-term Prognostic Value of Cardiac MRI Left Atrial Strain in ST-Segment Elevation Myocardial Infarction. Radiology 2020;296:299-309.
16. Leiner T, Bogaert J, Friedrich MG, Mohiaddin R, Muthurangu V, Myerson S, Powell AJ, Raman SV, Pennell DJ. SCMR Position Paper (2020) on clinical indications for cardiovascular magnetic resonance. J Cardiovasc Magn Reson 2020;22:76.
17. Vasquez M, Nagel E. Clinical indications for cardiovascular magnetic resonance. Heart 2019;105:1755-62.
18. Kihlberg J, Gupta V, Haraldsson H, Sigfridsson A, Sarvari SI, Ebbers T, Engvall JE. Clinical validation of three cardiovascular magnetic resonance techniques to measure strain and torsion in patients with suspected coronary artery disease. J Cardiovasc Magn Reson 2020;22:83.
19. Alfuhied A, Marrow BA, Elfawal S, Gulsin GS, Graham-Brown MP, Steadman CD, Kanagala P, McCann GP, Singh A. Reproducibility of left atrial function using cardiac

magnetic resonance imaging. Eur Radiol 2021;31:2788-97.
20. Peters DC, Lamy J, Sinusas AJ, Baldassarre LA. Left atrial evaluation by cardiovascular magnetic resonance: sensitive and unique biomarkers. Eur Heart J Cardiovasc Imaging 2021;23:14-30.
21. Blume GG, Mcleod CJ, Barnes ME, Seward JB, Pellikka PA, Bastiansen PM, Tsang TS. Left atrial function: physiology, assessment, and clinical implications. Eur J Echocardiogr 2011;12:421-30.
22. Thygesen K, Alpert JS, Jaffe AS, Chaitman BR, Bax JJ, Morrow DA, White HD; . Fourth Universal Definition of Myocardial Infarction (2018). Circulation 2018;138:e618-51.
23. Deedwania P, Kosiborod M, Barrett E, Ceriello A, Isley W, Mazzone T, Raskin P; . Hyperglycemia and acute coronary syndrome: a scientific statement from the American Heart Association Diabetes Committee of the Council on Nutrition, Physical Activity, and Metabolism. Circulation 2008;117:1610-9.
24. Rodevan O, Bjornerheim R, Ljosland M, Maehle J, Smith HJ, Ihlen H. Left atrial volumes assessed by three- and two-dimensional echocardiography compared to MRI estimates. Int J Card Imaging 1999;15:397-410.
25. Yang Y, Yin G, Jiang Y, Song L, Zhao S, Lu M. Quantification of left atrial function in patients with non-obstructive hypertrophic cardiomyopathy by cardiovascular magnetic resonance feature tracking imaging: a feasibility and reproducibility study. J Cardiovasc Magn Reson 2020;22:1.
26. Petersen SE, Aung N, Sanghvi MM, Zemrak F, Fung K, Paiva JM, Francis JM, Khanji MY, Lukaschuk E, Lee AM, Carapella V, Kim YJ, Leeson P, Piechnik SK, Neubauer S. Reference ranges for cardiac structure and function using cardiovascular magnetic resonance (CMR) in Caucasians from the UK Biobank population cohort. J Cardiovasc Magn Reson 2017;19:18.
27. Lu ML, De Venecia T, Patnaik S, Figueredo VM. Atrial myocardial infarction: A tale of the forgotten chamber. Int J Cardiol 2016;202:904-9.
28. Dziewierz A, Giszterowicz D, Siudak Z, Rakowski T, Dubiel JS, Dudek D. Admission glucose level and in-hospital outcomes in diabetic and non-diabetic patients with acute myocardial infarction. Clin Res Cardiol 2010;99:715-21.
29. Paolisso P, Foà A, Bergamaschi L, Donati F, Fabrizio M, Chiti C, Angeli F, Toniolo S, Stefanizzi A, Armillotta M, Rucci P, Iannopollo G, Casella G, Marrozzini C, Galiè N, Pizzi C. Hyperglycemia, inflammatory response and infarct size in obstructive acute myocardial infarction and MINOCA. Cardiovasc Diabetol 2021;20:33.
30. Ceriello A. Cardiovascular effects of acute hyperglycaemia: pathophysiological underpinnings. Diab Vasc Dis Res 2008;5:260-8.
31. Høfsten DE, Løgstrup BB, Møller JE, Pellikka PA, Egstrup K. Abnormal glucose metabolism in acute myocardial infarction: influence on left ventricular function and prognosis. JACC Cardiovasc Imaging 2009;2:592-9.
32. Pepe M, Addabbo F, Cecere A, Tritto R, Napoli G, Nestola PL, Cirillo P, Biondi-Zoccai G, Giordano S, Ciccone MM. Acute Hyperglycemia-Induced Injury in Myocardial Infarction. Int J Mol Sci 2024;25:8504.
33. Kawel-Boehm N, Bremerich J. The Importance of Left Atrial Function after Myocardial Infarction. Radiology 2020;296:310-1.
34. Mangion K, Carrick D, Carberry J, Mahrous A, McComb C, Oldroyd KG, Eteiba H, Lindsay M, McEntegart M, Hood S, Petrie MC, Watkins S, Davie A, Zhong X, Epstein FH, Haig CE, Berry C. Circumferential Strain Predicts Major Adverse Cardiovascular Events Following an Acute ST-Segment-Elevation Myocardial Infarction. Radiology 2019;290:329-37.
35. Chung JW, Park YS, Seo JE, Son Y, Oh CW, Lee CH, Nam JH, Lee JH, Son JW, Kim U, Park JS, Won KC, Shin DG. Clinical Impact of Dysglycemia in Patients with an Acute Myocardial Infarction. Diabetes Metab J 2021;45:270-4.
36. Pepe M, Zanna D, Cafaro A, Marchese A, Addabbo F, Navarese EP, Napodano M, Cecere A, Resta F, Paradies V, Bortone AS, Favale S. Role of plasma glucose level on myocardial perfusion in ST-segment elevation myocardial infarction patients. J Diabetes Complications 2018;32:764-9.
37. Schuster A, Backhaus SJ, Stiermaier T, Navarra JL, Uhlig J, Rommel KP, Koschalka A, Kowallick JT, Lotz J, Gutberlet M, Bigalke B, Kutty S, Hasenfuss G, Thiele H, Eitel I. Left Atrial Function with MRI Enables Prediction of Cardiovascular Events after Myocardial Infarction: Insights from the AIDA STEMI and TATORT NSTEMI Trials. Radiology 2019;293:292-302.
38. Otani K, Takeuchi M, Kaku K, Haruki N, Yoshitani H, Tamura M, Abe H, Okazaki M, Ota T, Lang RM, Otsuji Y. Impact of diastolic dysfunction grade on left atrial mechanics assessed by two-dimensional speckle tracking echocardiography. J Am Soc Echocardiogr 2010;23:961-7.
39. Teo SG, Yang H, Chai P, Yeo TC. Impact of left ventricular diastolic dysfunction on left atrial volume and function: a volumetric analysis. Eur J Echocardiogr

2010;11:38-43.
40. Fontes-Carvalho R, Sampaio F, Teixeira M, Ruivo C, Ribeiro J, Azevedo A, Leite-Moreira A, Ribeiro VG. Left atrial deformation analysis by speckle tracking echocardiography to predict exercise capacity after myocardial infarction. Rev Port Cardiol (Engl Ed) 2018;37:821-30.
41. Wang X, Pabon MA, Cikes M, Jering K, Mullens W, Kober L, Jhund PS, Kovacs A, Merkely B, Zhou Y, McMurray JJV, Shah AM, Hegde SM, Claggett B, Pfeffer MA, Solomon SD. Sex differences in cardiac structure and function following acute myocardial infarction: Insights from the PARADISE-MI echocardiographic substudy. Eur J Heart Fail 2024. [Epub ahead of print]. doi: 10.1002/ejhf.3472.
42. Zareian M, Ciuffo L, Habibi M, Opdahl A, Chamera EH, Wu CO, Bluemke DA, Lima JA, Venkatesh BA. Left atrial structure and functional quantitation using cardiovascular magnetic resonance and multimodality tissue tracking: validation and reproducibility assessment. J Cardiovasc Magn Reson 2015;17:52.
43. Zhang R, Cui C, Wang S, Wang Y, Liu R, Liu L. Interaction effect of hypertension and obesity on left atrial phasic function: a three-dimensional echocardiography study. Quant Imaging Med Surg 2023;13:4463-74.
44. Davarpasand T, Hosseinsabet A, Omidi F, Mohseni-Badalabadi R. Interaction effect of myocardial infarction and obesity on left atrial functions. J Clin Ultrasound 2021;49:431-41.

Cite this article as: Han PL, Li K, Jiang Y, Jiang L, Tang X, Guo YK, Li Y, Yang ZG. Left atrioventricular coupling and left atrial abnormality in patients with acute myocardial infarction with and without hyperglycemia assessed with 3.0T cardiac magnetic resonance imaging feature tracking. Quant Imaging Med Surg 2025;15(3):2347-2361. doi: 10.21037/qims-24-1757

